Ameliorative Effects of Selenium and Vitamins C and E on Chronic Fluoride Pancreatic Toxicity: Structural and Ultrastructural Changes in Albino Rats

Gamal Abdel Salam[1], Esam M. Mehlab[1], Mohamed Al-Shishtawy[2] and Ibrahim Al-Zahrani[3]

Departments of Anatomy[1]and Forensic & Applied Toxicology[2], Faculty of Medicine, Benha University, Egypt and Pathology, Faculty of Medicine, Northern Border University, KSA[3]

Abstract: Objectives: Histological evaluation of toxic effects of chronic exposure to sodium fluoride (NaF) on pancreas of albino rats and the impact of synchronous administration of selenium and vitamins C and E. **Materials & Methods:** The study comprised 60 normal healthy growing adult male albino rats, weighing 200-250 gm. The animals were divided into three equal groups: Control group received no medications, NaF group received NaF solution in a dose of 10 mg/kg body weight (BW) once daily for 35 days. Prophylaxis group received one daily dose of NaF solution in addition to selenium and vitamins C and E. All medications were administered orally using syringe connected to a 8F pediatric feeding tube. Studied animals were weighed daily for adjustment of the doses of used medications. After 35 days from the beginning of experiment all animals were sacrificed and pancreas was extracted for light microscopic (LM) examination of specimens stained with hematoxilin-eosin (Hx & E) and Masson's trichrome stain and for electron microscopic examination. **Results:** The percentage of BW gain was significantly higher in control group compared to other groups with significantly higher percentage of BW gain in prophylaxis group compared to NaF group. LM examination of NaF group specimen showed loss of normal architecture of pancreatic acini with the appearance of many cytoplasmic vacuoles. There is congestion of blood vessels (BV) with occasional extravasations between acinar cells. Focal condensation of CT around the congested BV and in between acini. In prophylaxis group, architecture of pancreatic acini was preserved with basal nuclei and apical zymogen granules. Dark and light cells of islets of Langerhans appeared normal with minimal congestion of BV. Masson's Trichrome stained sections showed condensation of connective tissue around BV with less CT in between acini. EM examination of NaF group specimen showed pyramidal acinar cells containing rounded basal heterochromatic nuclei and well defined rough endoplasmic reticulum (rER). Some mitochondria are intact, while others are vacuolated with small number of zymogen granules. There were multiple vesicles of variable sizes with large vesicles having membranous structures and amorphous materials. Nuclei of B-cell of islet of Langerhans were heterochromatic and its characteristic granules are normal with central dense core separated from their limiting membrane by clear space, while other granules are vacuolated. In prophylaxis group, specimens showed that some pyramidal acinar cell had double nuclei and its cytoplasm contains rER, many zymogen granules and some vesicles. B-cell had heterochromatic nucleus and its characteristic granules had a dense core. A-cell had oval nucleus with moderate amount of electron dense granules. **Conclusion:** Chronic fluoride exposure had deleterious effect on pancreatic structure and ultrastructure with manifested failure to thrive. Such effects could be attributed to redox state disturbances and could be ameliorated with the use of selenium and vitamins C and E.

[Gamal Abdel Salam, Esam M. Mehlab, Mohamed Al-Shishtawy and Ibrahim Al-Zahrani. **Ameliorative Effects of Selenium and Vitamins C and E on Chronic Fluoride Pancreatic Toxicity: Structural and Ultrastructural Changes in Albino Rats.** *J Am Sci* 2013;9(3):274-283]. (ISSN: 1545-1003). http://www.jofamericanscience.org. 38

Kew words: Fluoride, Pancreas, Structural changes, Ultrastructure changes, Selenium, Vitamins.

1. Introduction

Pancreas is a compound, finely nodular gland that is a mixed exocrine (about 80%) and endocrine (about 20%) organ. The endocrine portion consists of the islets of Langerhans, which are spherical clusters of light-staining cells scattered throughout the pancreas. The exocrine portion consists of numerous dark-staining acini composed of tubular and spherical masses of cells, which are the subunits of the lobule **(Kuehnel, 2003; Young *et al.*, 2006)**.

The lumen of the acinus contains centroacinar cells, which are unique to the pancreas and appear as pale staining and smaller than the acinar cells. The lumen of the acinus leads into the intralobular ducts, which are covered by low columnar epithelial cells. Goblet cells and occasional argentaffin cells also are present. The interlobular ducts anastomose to become the main pancreatic duct. Acinar cells are tall, pyramidal or columnar epithelial cells, with their broad bases on a basal lamina and their apices converging on a central lumen. The basal portion of the cells contains one or two centrally located, spherical nuclei and extremely basophilic cytoplasm. The Golgi complex lies between the nucleus and zymogen granules. The acinar cell has several short, slender microvilli about 0.2 µm in length that extend into the lumen of the acinus **(Michael, 2006, Ovalle & Nahirney, 2008)**.

Thin filaments form the axis of the microvilli as well as a network beneath the apical plasmalemma. These microfilaments apparently play a structural role because their disruption causes expansion of the acinar lumen and loss of microvilli. Adjacent cells are joined at the apical surface by electron-dense intercellular junctions. Tight junctions form a belt-like band around the apical end of the cell and are produced by the apposition of the external membrane leaflets of neighboring cells. These junctions prevent the reflux of secreted substances from the duct into the intercellular space **(Mescher, 2010)**.

Fluoride is an ubiquitous element in the environment and has a remarkable prophylactic effect at low concentrations by inhibiting dental caries, while at higher concentrations it causes dental and skeletal fluorosis. Endemic fluorosis is prevalent in many parts of the world and causes damage not only to hard tissues of teeth and skeleton, but also to soft tissues, such as brain, liver, kidney, and spinal cord **(Chachra *et al.*, 2008; Ozsvath, 2009)**.

Epidemiological investigations reveal that intelligence quotient of children living in endemic fluorosis areas is lower than that of children living in low fluoride areas. It has been demonstrated that high concentrations of fluoride can decrease learning ability and memory in some animal experiments and result in dysfunctions of the central nervous system **(Xiang *et al.*, 2003; Wang *et al.*, 2007; Ozsvath *et al.*, 2009)**.

As the cases of many chronic degenerative diseases, the increase of reactive oxygen species (ROS) and lipid peroxidation (LPO) has been considered to play an important role in the pathogenesis of chronic fluoride toxicity. Thus, the current study aimed to evaluate the histological toxic effects of chronic exposure to sodium fluoride (NaF) on pancreas of albino rats and the impact of synchronous administration of selenium and vitamins C and E as antioxidant therapy.

2. Materials & Methods

Animals

The study comprised 60 normal healthy growing adult male albino rats, weighing 200-250 gm. Rats were purchased from the laboratories of Ministry of Agriculture, and kept under standard conditions, temperature 20^{o}C, humidity 60% and 12-hs day/night cycle, and maintained on standard diet and free water supply till the start of study regimens.

Drugs

1- Sodium fluoride (NaF, El-Gomhoria Co. for Chemical Products, Al-Amyeria, Cairo, Egypt) was purchased as NaF powder which is white water-soluble powder. Each gram of NaF was dissolved in 100 ml of distilled water to obtain a solution of concentration of 10 mg NaF/ml water. Freshly prepared solution was provided as once daily oral dose of 10 mg/kg body weight **(Błaszczyk *et al.*, 2008)**.
2- Sodium selenite was dissolved in distilled water and was given as once daily oral dose of 25 µg in 1 ml distilled water/kg body weight **(Shivarajashankara *et al.*, 2003)**.
3- Vitamin C was dissolved in distilled water and was given as once daily oral dose of 50 mg in 1 ml distilled water/kg body weight **(Reddy *et al.*, 2003)**.
4- Vitamin E was dissolved in olive oil and was given as once daily oral dose of 10 mg in 1 ml olive oil/kg body weight **(Mittal & Flora, 2007)**.

Study Protocol

The animals were divided into the following study groups (each in a separate cage) according to medication used:

1. Control group included 20 rats kept on normal diet without medications.
2. Sodium fluoride group (NaF group) included 20 rats received NaF solution only for 35 days.
3. Prophylaxis group included 20 rats received one oral daily dose of NaF solution in addition to selenium and vitamins C & E. Doses were calculated according to animal's body weight and was given as a part of one ml/day for 35 days.

All medication were administered orally using syringe connected to a 8F pediatric feeding tube to assure consumption of the total calculated dose. Studied animals were weighed daily for adjustment of the doses of used medications. After 35 days from the beginning of experiment, final body weight was determined and the percentage of body gain was calculated as the difference between body weight at the end and start of the study divided by the initial weight and multiplied by 100.

Then, both control and study groups were sacrificed by inhalation of high dose of ether. The abdomen was explored, the pancreas was identified at the concavity of the duodenum, and was meticulously dissected and extract.

For light microscopic examination, liver specimen were fixed in 10% buffered formalin, (pH 7.8) and, then thin sections (4 µm) were stained with hematoxilin-eosin (HE) for general histological features determination **(Bancroft & Gamble, 2002)**, Masson's trichrome stain was used for connective tissue staining **(Leong, 1996)**. Specimens for electron microscopic examination were immersed in 2.5% gluteraldehyde buffered with 0.1 M phosphate buffer for 2 hours at room temperature, then post-fixed in 1% osmium tetroxide for 2 hours at 4^{o}C. After fixation,

dehydration with ascending grades of ethanol was performed; specimens were cleared in propylin oxide, embedded in epoxy resin and sectioned with ultramicrotome **(Hayat, 2000)**.

3. Results

At time of start of the study, mean initial body weight showed non-significant difference between study groups. On the 35th day, the final body weight was significantly (p<0.001) higher in all groups compared to initial body weight with significantly (p <0.001) higher final body weight in control and prophylaxis groups compared to NaF group and non-significantly higher final body weight in control versus prophylaxis group. However, the percentage of weight gain throughout the study period was significantly higher in control group compared to NaF group (p <0.001) and prophylaxis group (p =0.015) with significantly (p <0.001) higher percentage of body weight gain in prophylaxis group compared to NaF group, (Table 1, Fig. 1).

Table (1): Mean body weight of studied animals determined at start and end of the study and the percentage of change

			Control group	NaF group	Prophylaxis group
Initial body weight (gm)	Weight		216±13.2 (200-250)	212.5±9.2 (200-230)	214±9.7 (200-230)
	Statistical analysis	Z=		0.872	0.405
		P_1		>0.05	>0.05
		Z=			1.289
		P_2			>0.05
Final body weight (gm)	Weight		249.5±15.4 (220-280)	224.1±11.1 (207-241)	240.6±12.3 (213-266)
	Statistical analysis	Z=	3.936	3.927	3.921
		P_3	<0.001	<0.001	<0.001
		Z=		3.529	1.680
		P_1		<0.001	>0.05
		Z=			3.847
		P_2			<0.001
% of change	Percentage		15.6±4.4 (7.1-21.4)	5.4±1.5 (3.5-9.5)	12.4±3.9 (4.4-19.1)
	Statistical analysis	Z=		3.932	2.427
		P_1		<0.001	=0.015
		Z=			3.845
		P_2			<0.001

Date are presented as mean±SD; ranges are in parenthesis

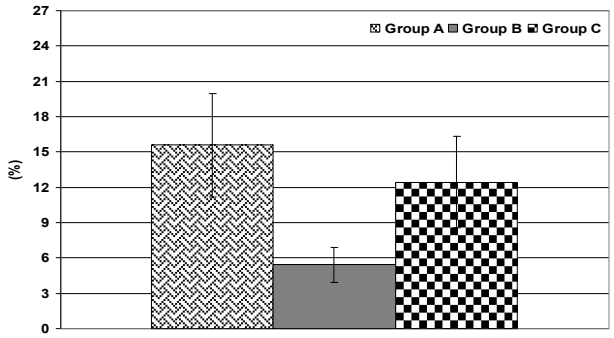

Fig. (1): Mean (±SD) percentage of body weight change at the end of the study in relation to weight at start of study

Light microscopic findings

Control group

In Hx & E stained sections, control rat showed normal pancreatic architecture. Pancreatic lobules consisted of closely packed acini of different sizes and shapes and were separated by interlobular connective tissue (CT) that contains pancreatic ducts and blood vessels (Fig. 2). The cells lining pancreatic acini are pyramidal in shape with basal deeply stained nucleus and some cells have doubled nuclei with the apical part contained zymogen granules, (Fig. 3). Islets of Langerhans were surrounded by pancreatic acini and interlobular ducts were lined by flat cells, (Fig. 4). Islets of Langerhans appeared consisting of cells arranged in circular groups and variable in sizes. A-cells have oval and dark nuclei, while B-cells have rounded and pale nuclei and blood capillaries are embedded in between the cells, (Fig. 5). Masson's Trichrome stained sections showed more CT around blood vessels (BV) with minimal CT are seen between the pancreatic acini, (Fig. 6).

NaF group

In fluoride-treated rat, Hx & E stained sections showed loss of normal architecture of pancreatic acini with the appearance of many cytoplasmic vacuoles of variable sizes, (Fig. 7). There is congestion of blood vessels with blood cells inside it with occasional extravasations of blood in the interlobular spaces and between acinar cells, (Fig. 8). Masson's Trichrome stained sections showed focal condensation of CT around the congested blood vessels and in between acini, (Fig. 9).

Prophylaxis group

In prophylaxis group, Hx & E stained sections showed intact pancreatic acini and islets of

Langerhans, (Fig. 10). Moreover, the architecture of pancreatic acini is preserved with basal nuclei and apical zymogen granules, but few cells contain vacuoles, (Fig. 11). Dark and light cells of islets of Langerhans appeared normal with minimal congestion of blood vessels, (Fig. 12). Masson's Trichrome stained sections showed condensation of connective tissue around blood vessels with less CT in between acini, (Fig. 13). Some acini showed complete degeneration, while others are vacuolated, but islets of Langerhans are intact, (Fig. 14).

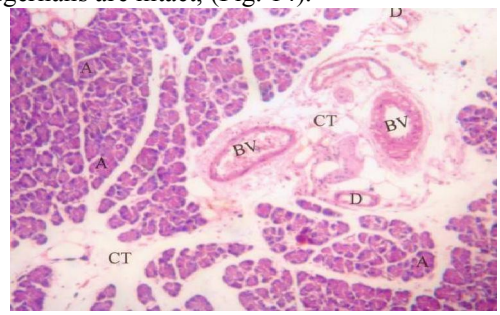

Fig. (2): A photomicrograph of an adult control rat pancreas showing: Pancreatic lobules consisting of closely packed acini (A) of different sizes and shapes separated by interlobular connective tissue (CT) that contains pancreatic ducts (D) and blood vessels (BV). (Hx & E x400)

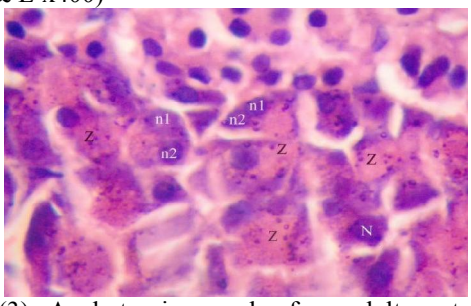

Fig. (3): A photomicrograph of an adult control rat pancreas showing: The cells lining pancreatic acini. Each cell is pyramidal in shape with basal deeply stained nucleus (N). Some cells have doubled nuclei (n1, n2). Apical part of the acinar cell contains zymogen granules (Z). (Hx & E x400)

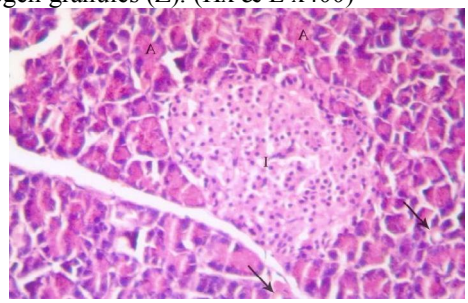

Fig. (4): A photomicrograph of an adult control rat pancreas showing: An islet of Langerhans (I) surrounded by pancreatic acini (A). The interlobular ducts (arrow) are lined by flat cells. (Hx & E x100)

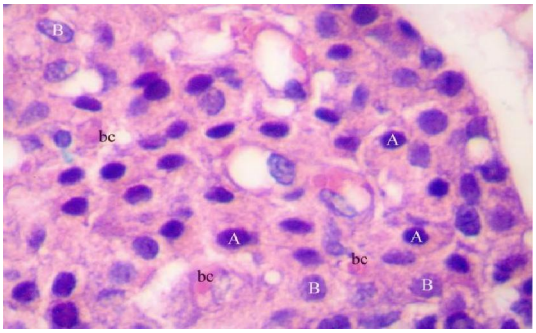

Fig.(5): A photomicrograph of an adult control rat pancreas showing: The structure of an islet of Langerhans consisting of cells arranged in circular groups and variable in sizes. The A-cells (A) have oval and dark nuclei. B-cells (B) have rounded and pale nuclei. Blood capillaries (bc) are embedded in between the cells. (Hx & E x400)

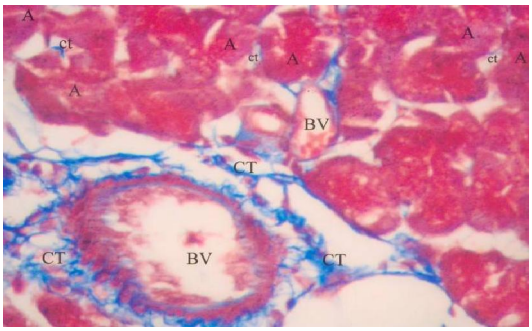

Fig. (6): A photomicrograph of an adult control rat pancreas showing: Dense connective tissue (CT) around blood vessels (BV) and minimal connective tissue (ct) are seen between the pancreatic acini (A). (Masson's Trichrome x 200)

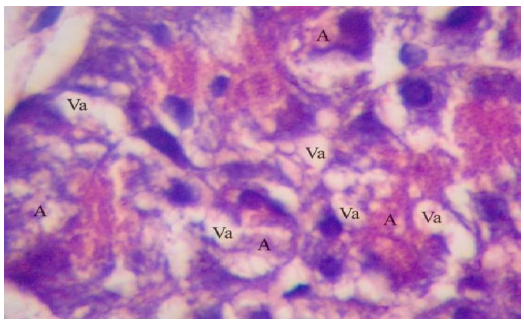

Fig. (7): A photomicrograph of an adult rat pancreas in NaF group showing complete loss of normal architecture of pancreatic acini (A) with appearance of many cytoplasmic vacuoles (Va) of variable sizes. (Hx & E x 400)

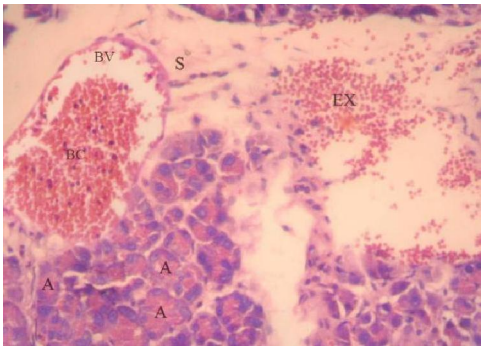

Fig. (8): A photomicrograph of an adult rat pancreas in NaF group showing congestion of blood vessels (BV) with blood cells (BC) and extravasations (EX) of blood in the interlobular spaces (S), but pancreatic acini (A) appeared intact. (Hx & E x100)

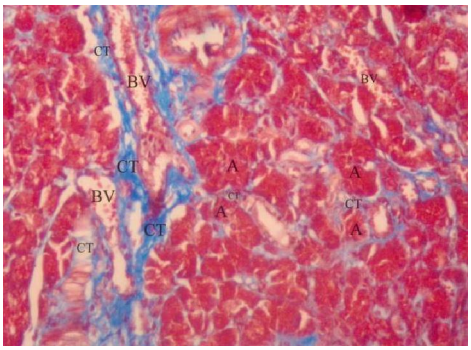

Fig. (9): A photomicrograph of an adult rat pancreas in NaF group showing focal condensation of connective tissue (CT) around the congested blood vessels (BV) and in between acini (A). (Masson's Trichrome x 100)

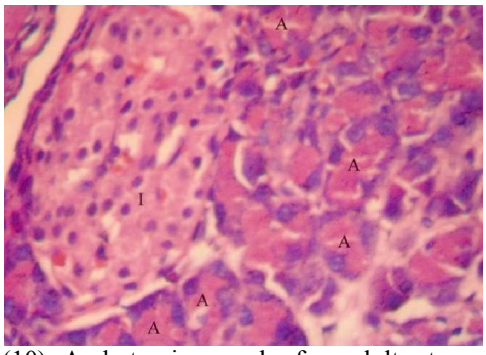

Fig. (10): A photomicrograph of an adult rat pancreas in prophylaxis group showing intact pancreatic acini (A) and islet of Langerhans (I). (Hx & E x200)

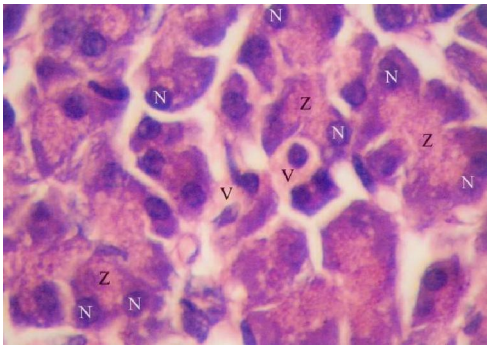

Fig. (11): A photomicrograph of an adult rat pancreas in prophylaxis group showing apparently normal architecture of pancreatic acini with basal nuclei (N) and apical zymogen granules (Z). Few cells contain vacuoles (V). (Hx & E x400)

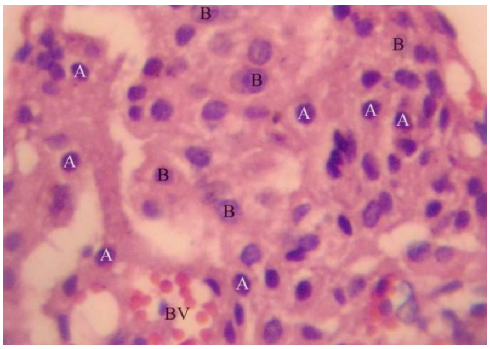

Fig. (12): A photomicrograph of an adult rat pancreas in prophylaxis group showing dark (A) and light (B) cells of Langerhans. Some blood vessels (BV) are congested with RBCs. (HX&E x 400)

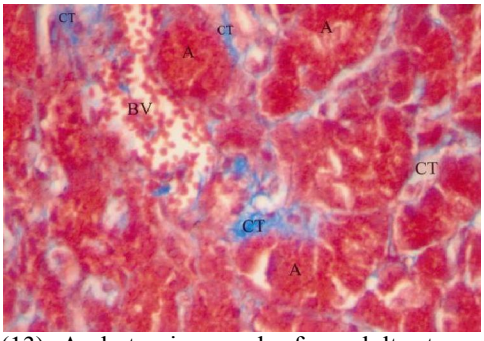

Fig. (13): A photomicrograph of an adult rat pancreas in prophylaxis group showing connective tissue (CT) is more condensed around the blood vessels (BV) and less amount in-between the acini (A). (Masson's Trichrome x 200)

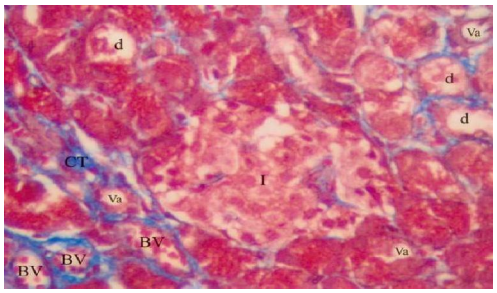

Fig. (14): A photomicrograph of an adult rat pancreas in prophylaxis group showing moderate amount of connective tissue (CT) around the blood vessels (BV), and few amount of connective tissue in-between the acini. Some acini show complete degeneration (d), while others are vacuolated (Va). Islet of Langerhans (I) is intact. (Masson's Trichrome x 200)

Electron microscopic examination

Control group

Examined specimens showed normal junctional complexes between the cells of pancreatic acinus. The cytoplasm contains closely packed cisternae of rough endoplasmic reticulum (rER) and mitochondria and heterochromatic nucleus, (Fig. 15). Nuclei of acinar cells were rounded heterochromatic and surrounded by intact mitochondria, zymogen granules and cisternae of rER, (Fig. 16). B-cells of islet of Langerhans showed heterochromatic nucleus. The core of the characteristic granules of B-cells of islet of Langerhans is pleomorphic with a wide clear space between the core and the outer limiting membrane of the granules, (Fig. 17). A-cell of islet of Langerhans showed heterochromatic nucleus and its characteristic granules were rounded with dense cores, (Fig. 18).

NaF group

Examined specimens showed pyramidal acinar cell containing rounded basal heterochromatic nucleus and well defined rER. Some cisternae of ER are circular in form. Some mitochondria (M) are intact, while others are vacuolated. There was small number of zymogen granules and centroacinar cells showed elongated nucleus, (Fig. 19). Some acinar cells have two nuclei which are heterochromatic. Also, there were multiple vesicles of variable sizes with large vesicles having membranous structures and amorphous materials, (Fig. 20). Nuclei of B-cell of islet of Langerhans were heterochromatic. Some of B-cell characteristic granules are normal with central dense core separated from their limiting membrane by clear space, while other granules are vacuolated , (Fig. 21).

Prophylaxis group

Examined specimens showed that some pyramidal acinar cell had double nuclei and its cytoplasm contains rER, many zymogen granules and some vesicles, (Fig. 22). B-cell of islet of Langerhans had heterochromatic nucleus and its characteristic granules had a dense core separated from the surrounding membrane by a light zone with some granules are vacuolated, (Fig. 23). A-cell of islet of Langerhans showed oval nucleus with moderate amount of electron dense granules , (Fig. 24).

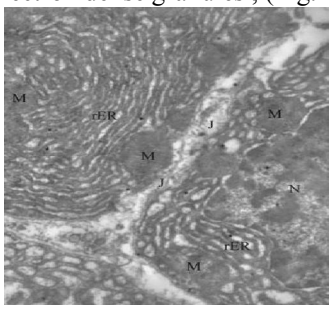

Fig. (15): An electron photomicrograph of an adult control rat pancreas showing junctional complexes (J) between the cells of pancreatic acinus. The cytoplasm contains closely packed cisternae of rough endoplasmic reticulum (rER) and mitochondria (M) and heterochromatic nucleus (N). (EM x10,000)

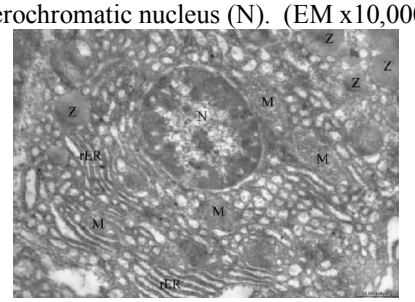

Fig. (16): An electron photomicrograph of an adult control rat pancreas showing a part of acinar cell with rounded heterochromatic nucleus (N) which is surrounded by intact mitochondria (M), zymogen granules (Z) and cisternae of rough endoplasmic reticulum (rER). (EM x10,000)

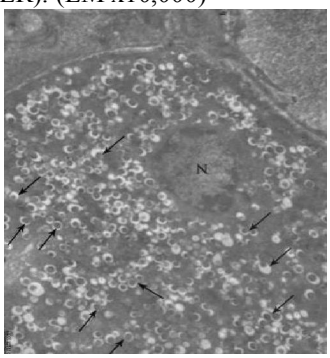

Fig. (17): An electron photomicrograph of an adult control rat pancreas showing B-cells of islet of Langerhans with its heterochromatic nucleus (N) and characteristic granules (arrow). The core of the granules is pleomorphic and a wide clear space is noted between the core and the outer limiting membrane of the granules. (EM x10,000)

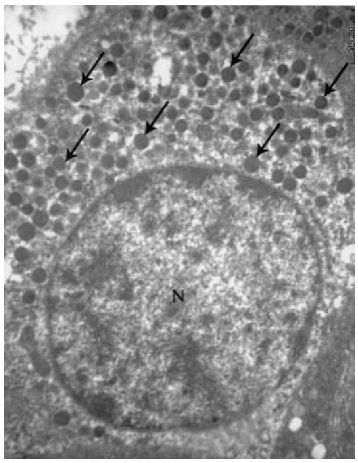

Fig. (18): An electron photomicrograph of an adult control rat pancreas showing A-cell of islet of Langerhans with its heterochromatic nucleus (N) and characteristic granules with rounded dense cores (Arrow). (EM x10,000)

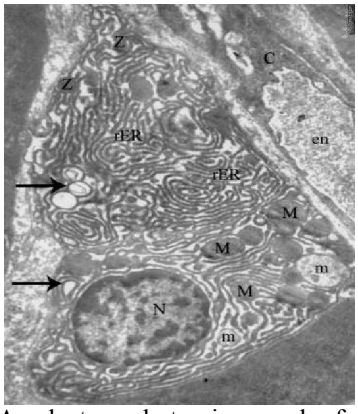

Fig. (19): An electron photomicrograph of an adult rat pancreas of NaF group showing pyramidal acinar cell containing rounded basal heterochromatic nucleus (N), well defined rough endoplasmic reticulum (rER) with some cisternae are circular in their forms (Arrow). Some mitochondria (M) are intact, while others are vacuolated (m). Zymogen granules (z) are few and centroacinar cell (c) with elongated nucleus (en). (EM x6000)

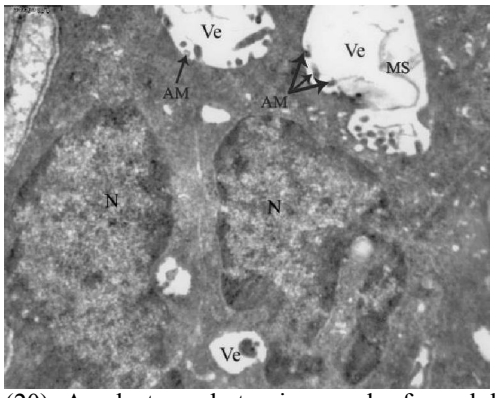

Fig. (20): An electron photomicrograph of an adult rat pancreas of NaF group showing an acinar cell with two heterochromatic nuclei (N). There are multiple small and large sized vesicles (Ve). Large vesicles have membranous structures (MS) and amorphous materials (AM). (EM 10,000)

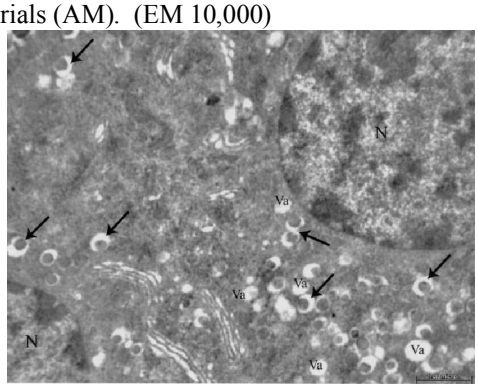

Fig. (21): An electron photomicrograph of an adult rat pancreas of NaF group showing parts of two B-cell of islet of Langerhans with heterochromatic nuclei (N) and characteristic granules. Some granules are normal with central dense core separated from their limiting membrane by clear space (arrow), while other granules are vacuolated (Va). (EM x10,000)

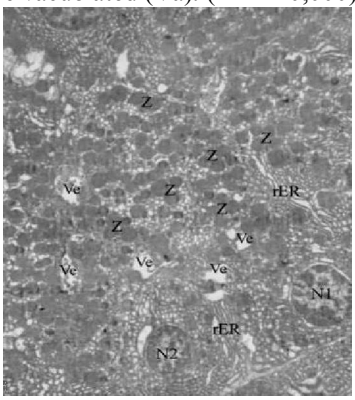

Fig. (22): An electron photomicrograph of an adult rat pancreas of prophylaxis group showing pyramidal acinar cell with double nuclei (N1, N2). Its cytoplasm contains rough endoplasmic reticulum (rER), many zymogen granules (Z) and some vesicles (Ve). (EM x3000)

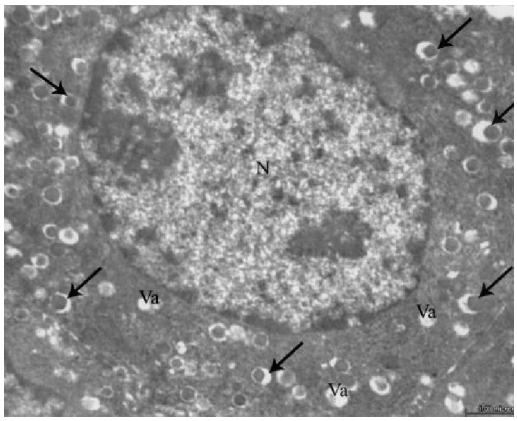

Fig. (23): An electron photomicrograph of an adult rat pancreas of prophylaxis group showing B-cell of islet of Langerhans with heterochromatic nucleus (N). The characteristic granules have a dense core separated from the surrounding membrane by a light zone (arrow). Some granules are vacuolated (Va). (EM x10,000)

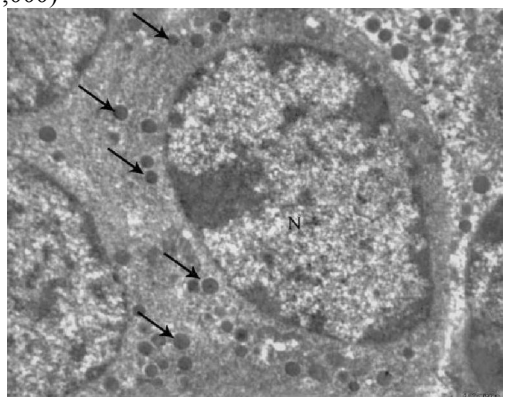

Fig. (24): An electron photomicrograph of an adult rat pancreas of prophylaxis group showing A-cell of islet of Langerhans with oval nucleus (N) and moderate amount of electron dense granules (arrow). (EM x10,000)

4.Discussion

In the current study, the percentage of BW gain was significantly higher in control group compared to NaF and prophylaxis group with significantly higher percentage of BW gain in prophylaxis compared to NaF group. These findings illustrated the impact of fluoride exposure on the ability to thrive despite being variable according to the use of prophylaxis or not. This decrease in the BW gain can be attributed to decreased appetite and consequently decreased consumption of feed and water, which ultimately lead to poor growth rate. Moreover, the decrease found in body weight gain could be due to primary malnutrition caused by fluoride by displacing other nutrients present in the diet (minerals/elements) and secondary malnutrition too results either from mal-digestion or mal-absorption of nutrients. In addition, gastrointestinal complications could have altered nutritional abilities and deficiencies virtually on all the nutrients. In support of these attributions, the significant difference in body weight gain between animals received selenium and vitamins compared to those did not receive prophylaxis.

These data are in line with that previously reported in literature; **Verma & Guna-Sherlin (2002)** found significant amelioration in BW and feed consumption in rats on administration of vitamin E. **Basha & Sujitha (2011)** observed decreased feed and water consumption, organ somatic index and marginal drop in body growth rate of rats exposed to high fluoride for two generations. **Shankar *et al.*(2012)** reported significantly reduced food efficiency ratio, BW gain, fecal fluoride excretion, serum calcium and increased bone fluoride deposition in animals maintained on fluoride in diet and concluded that chronic fluoride toxicity can interfere with calcium absorption by down-regulating S100G expression irrespective of calcium nutrition.

Histological examination of pancreatic specimens of animals exposed to NaF only showed loss of normal architecture of pancreatic acini, appearance of many cytoplasmic vacuoles of variable sizes with congestion of blood vessels and occasional extravasations of blood in the interlobular spaces and between acinar cells and focal condensation of CT around blood vessels and in between acini. These changes indicated disturbed exocrine functions of pancreas which are responsible for digestion of proteins and carbohydrates in duodenum thus indicating the concomitant mal-digestion which leads to failure to gain weight. In support of these data, in animals received prophylaxis, specimens showed preserved architecture of pancreatic acini with apical zymogen granules less CT in between acini.

These histological changes and the reported ameliorative effect of selenium and vitamins E and C on fluoride toxicity go in hand with that previously reported by **Yu *et al.*(2006)** who found NaF induced oxidative stress and apoptosis, and changes the cell cycle in rat renal cells and selenium and zinc antagonize oxidative stress, apoptosis, and cell cycle changes induced by excess fluoride.

Guney *et al.* (2007 a&b) reported decreased levels of endometrial malondialdehyde (MDA) with significant increase of antioxidant enzymatic activities on administration of vitamin C and E with fluoride treatment. Moreover, they reported that vitamins provided histopathological protection against fluoride induced endometrial damage and concluded that oxidative endometrial damage plays an important role in fluoride-induced endometrial toxicity, and the modulation of oxidative stress with vitamins reduces

this damage both at the biochemical and histological levels**. Matsui *et al.* (2007)** found NaF increased intracellular Ca^{2+} concentration and significantly increased the population of shrunken cells which are known to as parameters for early stage of apoptosis and concluded that NaF induces necrosis, associated with some apoptotic changes.

Stawiarska-Pięta *et al.*(2009), found that pathomorphological examinations of the lungs of animals received NaF revealed the appearance of erythrorrhagia, hyperaemia, necrosis of epithelium cells, numerous macrophages in interalveolar septa, infiltrations in the area of blood vessels and emphysematous blebs. Focal vacuolar degeneration cells and inflammatory infiltrations appeared only in pancreata and that the administration of vitamins A and E and coenzyme Q has a counteracting influence upon the degenerative changes seen in the examined organs.

Khalili & Biloklytska, (2009) reported elevated MDA, a lipid peroxidation product, and unsteady ratios of oxidized to reduced nicotinamide adenine dinucleotide reflected significant alterations in the redox state (RS) status in tissues specimens of animals exposed to oral fluoride alone compared to that received fluoride and vitamins or combination of vitamins and minerals and concluded that the combination of vitamins and minerals supplementation proved to restore MDA content and establish steady RS status. **Kumar *et al.*(2012)**, found that combined vitamin D and E treatment induced a significant improvement in reproductive functions affected by fluoride. **Stawiarska-Pięta *et al.*(2012)**, reported that the administration of antioxidants counteracted changes in the activity of the enzymes and the morphological abnormalities of the liver induced by NaF.

Electron microscopic examination of pancreatic specimens of NaF exposed animals showed that some cisternae of ER are circular in form, some mitochondria are intact, while others are vacuolated and small number of zymogen granules and centroacinar cells showed elongated nucleus. On contrary, specimens of prophylaxis group showed that some pyramidal acinar cell had double nuclei and its cytoplasm contains rER, many zymogen granules and some vesicles. These ultrastructural changes support that obtained by light microscopic examination and point to a fact that the deleterious effects of fluoride did not affect the cellular configurations only but extend to affect their cytoplasmic organelles and so affects their functions.

In trial to explore these changes, **Ito *et al.*(2009)** observed intracisternal granule, excessive autophagy and ribosomal degranulation in fluoride-exposed cells, occasionally with necrotic changes and concluded that these findings indicate that rER-stress by intracisternal granule accumulation lead to autophagy in exocrine pancreas cells and intense degranulation is a turning point that damaged cells change over from autophagy, cell-protective process, to cell-death process.

In conclusion; chronic fluoride exposure had deleterious effect on pancreatic structure and ultrastructure with manifested failure to thrive. Such effects could be attributed to redox state disturbances and could be ameliorated with the use of selenium and vitamins C and E.

References

1. Bancroft JD, Gamble M: Theory and practice of histological techniques. 5th ed., Churchill Livingstone. London, New York & Sydney, 2002; 377& 694.
2. Basha MP, Sujitha NS: Chronic Fluoride Toxicity and Myocardial Damage: Antioxidant Offered Protection in Second Generation Rats. Toxicol Int. 2011; 18(2): 99–104.
3. Błaszczyk I, Grucka-Mamczar E, Kasperczyk S, Birkner E: Influence of fluoride on rat kidney antioxidant system: effects of methionine and vitamin E. Biol Trace Elem Res. 2008; 121(1):51-9.
4. Chachra D, Vieira AP, Grynpas MD: Fluoride and mineralized tissues," Critical Reviews in Biomedical Engineering, 2008; 36(2-3): 183–223.
5. Guney M, Oral B, Demirin H, Karahan N, Mungan T, Delibas N: Protective effects of vitamins C and E against endometrial damage and oxidative stress in fluoride intoxication. Clin Exp Pharmacol Physiol. 2007a; 34(5-6):467-74.
6. Guney M, Oral B, Take G, Giray SG, Mungan T: Effect of fluoride intoxication on endometrial apoptosis and lipid peroxidation in rats: role of vitamins E and C. Toxicology. 2007b;231(2-3):215-23.
7. Hayat MA: Principals and Techniques of electron microscopy, 4th ed., Cambridge University, 2000; 96–123.
8. Ito M, Nakagawa H, Okada T, Miyazaki S, Matsuo S: ER-stress caused by accumulated intracistanal granules activates autophagy through a different signal pathway from unfolded protein response in exocrine pancreas cells of rats exposed to fluoride. Arch Toxicol. 2009; 83(2):151-9.
9. Khalili J, Biloklytska HF: Influence of supplementary vitamins and minerals on lipid peroxidation and redox state in heart, kidney and liver of rats exposed to fluoride. Fiziol Zh. 2009;55(6):75-80.

10. Kuehnel K: Color Atlas of Cytology, Histology and Microscopic Anatomy, 4th ed., 2003; 37 & 328.
11. Kumar N, Sood S, Arora B, Singh M, Beena, Roy PS: To Study the Effect of Vitamin D and E on Sodium-Fluoride-induced Toxicity in Reproductive Functions of Male Rabbits. Toxicol Int. 2012;19(2):182-7.
12. Leong AS: Principles and practice of medical laboratory sience. Volume 1: Basic Histotechnology. 1st ed., Philadelphia, Saunders Co., 1996; 171.
13. Matsui H, Morimoto M, Horimoto K, Nishimura Y: Some characteristics of fluoride-induced cell death in rat thymocytes: cytotoxicity of sodium fluoride. Toxicol In Vitro. 2007;21(6):1113-20.
14. Mescher AL: The Digestive Tract: In: Junqueira's Basic Histology, Text and Atlas, 12th ed., MC Graw – Hill, New York, Chicago, London, Toronto, Singapore, 2010; 287–97.
15. Michael HR: Digestive System III: Liver, Gallbladder, and Pancreas. In: Histology. A text and Atlas with Correlated Cell and Molecular Biology. 5th ed., Michael Hr, Wojciech P (eds), 2006; 576-90.
16. Mittal M, Flora SJ: Vitamin E supplementation protects oxidative stress during arsenic and fluoride antagonism in male mice. Drug Chem Toxicol. 2007;30(3):263-81.
17. Ovalle WK, Nahirney PC: In: Netter's Essential Histology, 1st ed., Saunders, China, Philadelphia, 2008; 324 –6.
18. Ozsvath DL: Fluoride and environmental health: a review. Reviews in Environmental Science and Biotechnology, 2009; 8(1): 59–79.
19. Reddy GB, Khandare AL, Reddy PY, Rao GS, Balakrishna N, Srivalli I: Antioxidant defense system and lipid peroxidation in patients with skeletal fluorosis and in fluoride-intoxicated rabbits. Toxicol Sci. 2003; 72(2):363-8.
20. Shivarajashankara YM, Shivashankara AR, Bhat PG, Rao SH: Lipid peroxidation and antioxidant systems in the blood of young rats subjected to chronic fluoride toxicity. Indian J Exp Biol. 2003; 41(8):857-60.
21. Shankar P, Ghosh S, Bhaskarachary K, Venkaiah K, Khandare AL: Amelioration of chronic fluoride toxicity by calcium and fluoride-free water in rats. Br J Nutr. 2012 Dec 11:1-10. [Epub ahead of print]
22. Stawiarska-Pieta B, Paszczela A, Grucka-Mamczar E, Szaflarska-Stojko E, Birkner E: The effect of antioxidative vitamins A and E and coenzyme Q on the morphological picture of the lungs and pancreata of rats intoxicated with sodium fluoride. Food Chem Toxicol. 2009; 47(10):2544-50.
23. Stawiarska-Pięta B, Bielec B, Birkner K, Birkner E: The influence of vitamin E and methionine on the activity of enzymes and the morphological picture of liver of rats intoxicated with sodium fluoride. Food Chem Toxicol. 2012;50(3-4):972-8.
24. Verma RJ, Guna-Sherlin DM. Sodium fluoride-induced hypoproteinemia and hypoglycemia in parental and F(1)-generation rats and amelioration by vitamin. Food Chem Toxicol. 2002;40:1781–8.
25. Wang SX, Wang ZH, Cheng XT, *et al.*: "Arsenic and fluoride expose in drinking water: children's IQ and growth in Shanyin Country, Shanxi Province, China," Environmental Health Perspectives, 2007; 115(4): 643–7.
26. Xiang Q, Liang Y, Chen Y, *et al.*: Effect of fluoride in drinking water on children's intelligence. Fluoride, 2003; 36(2): 84–94.
27. Young B, Lowe JS, Stevens A, Heath JW: Pancreas. In: Wheater's Functional Histology, Text and Color atlas, 5th ed., Churchill Livingstone, China, 2006; 293–5.
28. Yu RA, Xia T, Wang AG, Chen XM: Effects of selenium and zinc on renal oxidative stress and apoptosis induced by fluoride in rats. Biomed Environ Sci. 2006; 19(6):439-44.

1/28/2013